

RECEIVED  
DEC 17 1999  
OSTI

THE LIMIT OF THE FILM EXTRACTION TECHNIQUE FOR  
ANNULAR TWO-PHASE FLOW IN A SMALL TUBE

D. E. Helm and M. Lopez de Bertodano  
Purdue University

S. G. Beus  
Bettis Atomic Power Laboratory

DE-AC11-98PN38206

NOTICE

This report was prepared as an account of work sponsored by the United States Government. Neither the United States, nor the United States Department of Energy, nor any of their employees, nor any of their contractors, subcontractors, or their employees, makes any warranty, express or implied, or assumes any legal liability or responsibility for the accuracy, completeness or usefulness of any information, apparatus, product or process disclosed, or represents that its use would not infringe privately owned rights.

BETTIS ATOMIC POWER LABORATORY

WEST MIFFLIN, PENNSYLVANIA 15122-0079

Operated for the U.S. Department of Energy  
by Bechtel Bettis, Inc.

## **DISCLAIMER**

**This report was prepared as an account of work sponsored by an agency of the United States Government. Neither the United States Government nor any agency thereof, nor any of their employees, make any warranty, express or implied, or assumes any legal liability or responsibility for the accuracy, completeness, or usefulness of any information, apparatus, product, or process disclosed, or represents that its use would not infringe privately owned rights. Reference herein to any specific commercial product, process, or service by trade name, trademark, manufacturer, or otherwise does not necessarily constitute or imply its endorsement, recommendation, or favoring by the United States Government or any agency thereof. The views and opinions of authors expressed herein do not necessarily state or reflect those of the United States Government or any agency thereof.**

## **DISCLAIMER**

**Portions of this document may be illegible in electronic image products. Images are produced from the best available original document.**

## THE LIMIT OF THE FILM EXTRACTION TECHNIQUE FOR ANNULAR TWO-PHASE FLOW IN A SMALL TUBE

D. E. Helm and M. Lopez de Bertodano  
e-mail: bertodan@ecn.purdue.edu  
School of Nuclear Engineering  
Purdue University

S. G. Beus  
Bettis Atomic Power Laboratory

### ABSTRACT

The limit of the liquid film extraction technique was identified in air-water and Freon-113 annular two-phase flow loops. The purpose of this research is to find the limit of the entrainment rate correlation obtained by Lopez de Bertodano et. al. (1998). The film extraction technique involves the suction of the liquid film through a porous tube and has been widely used to obtain annular flow entrainment and entrainment rate data.

In our experiments there are two extraction probes. After the first extraction the entrained droplets in the gas core deposit on the tube wall. A new liquid film develops entirely from liquid deposition and a second liquid film extraction is performed. While it is assumed that the entire liquid film is removed after the first extraction unit, this is not true for high liquid flow. At high liquid film flows the interfacial structure of the film becomes frothy. Then the entire liquid film cannot be removed at the first extraction unit, but continues on and is extracted at the second extraction unit.

A simple model to characterize the limit of the extraction technique was obtained based on the

hypothesis that the transition occurs due to a change in the wave structure. The resulting dimensionless correlation agrees with the data.

### INTRODUCTION

The film extraction technique has been in use for many years to obtain entrainment data in annular two-phase flows. The purpose of this paper is to determine the limit of the liquid film extraction technique measurements obtained in air-water and Freon-113 loops.

First it is necessary to define the terms of ripple, frothy, and wispy annular flow. Bennett et. al. (1965-1966) refer to annular and wispy annular flow where each contains a "liquid film on the wall with a continuous gas core in the center of the channel". The distinction is that wispy annular flow has an entrained liquid that is agglomerated and in annular flow it is broken up into small droplets only. Figure 1 shows the film structure for low liquid film flow or ripple flow and Figure 2 shows the structure when the flow of the liquid film is high or frothy.

Because Hewitt and Bennett used X-ray photography and a high-speed camera within the tube

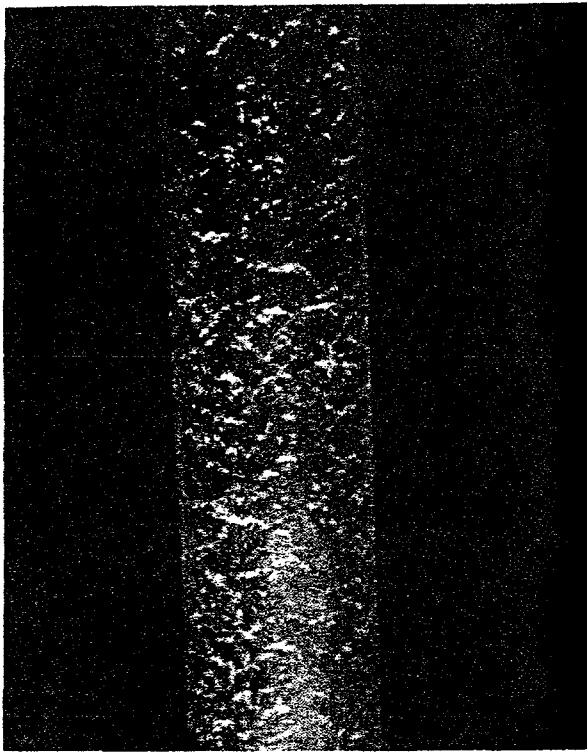


Figure 1: Ripple-annular flow

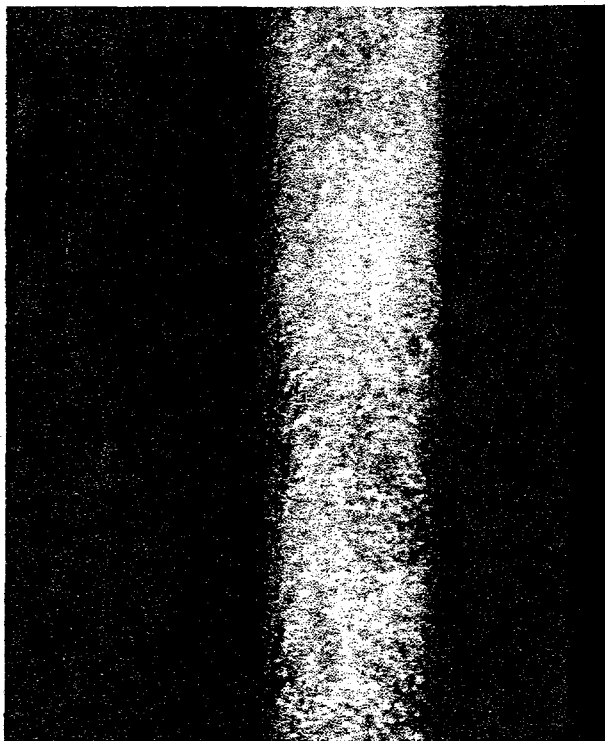


Figure 2: Frothy-annular flow

they were able to see the structure of the waves from the inside of the tubes and identify the wispy annular regime. The current study merely observed the flow patterns externally, and although there was a clear transition away from ripple annular flow, it is not possible to determine with confidence that this transition tube, they were able to see the structure of the waves was to the wispy annular regime. What can be stated with confidence is that the equipment identified a transition from ripple to frothy annular flow, and that visual observation verified this transition.

#### NOMENCLATURE

$C_i$	interfacial friction factor
$D$	tube diameter (m)
$h$	liquid film thickness (m)
$j_f$	volumetric flux of total liquid (m/s)
$j_g$	volumetric flux of total gas (m/s)
$j_{if}$	volumetric flux of liquid film (m/s)
$k_s$	wave height (m)
$N_{\mu f}$	viscosity number (equation 20)
$p$	pressure (Pa)
$Re_{if}$	Liquid film Reynolds number, $\rho_f j_{if} D / \mu_f$
$T$	temperature ( $^{\circ}\text{C}$ )
$u^*$	friction velocity equal to $[\tau_w / \rho]^{1/2}$ (m/s)
$We_g$	Weber number of the gas, $\rho_g j_g^2 D / \sigma$
$We_{if}$	Weber number of liquid film, $\rho_f j_{if}^2 D / \sigma$
$\dot{m}_g$	mass flow rate of the gas (kg/s)
$\dot{m}_f$	mass flow rate of the liquid film (kg/s)
$\dot{m}_{f1}$	mass flow rate from the first extraction
$\dot{m}_{f2}$	mass flow rate from the second extraction

#### Greek symbols

$\lambda$	wave length (m)
$\nu_f$	kinematic viscosity of liquid ( $\text{m}^2/\text{s}$ )
$\nu_g$	kinematic viscosity of gas ( $\text{m}^2/\text{s}$ )
$\rho_f$	liquid density ( $\text{kg}/\text{m}^3$ )
$\rho_g$	gas density ( $\text{kg}/\text{m}^3$ )
$\sigma$	surface tension (N/m)
$\tau$	shear stress ( $\text{N}/\text{m}^2$ )

## EXPERIMENTS

*Air-water loop:* The current experiments were made in an air-water and a Freon-113 loop. Although previous work has been done on air-water loops the main purpose for doing so in the current study was to develop the experimental techniques to be used on the more complex Freon loop. In addition, the data from the air-water loop provide a reference to compare the Freon data to.

The air-water test section is a 9.5 mm diameter vertical tube with adiabatic upward flow. The first extraction is 440 diameters from the inlet to ensure a fully developed film. Details of the air-water loop apparatus have been described by Lopez de Bertodano, Jan, and Beus (1997). Figure 3 shows a schematic of the air-water test section. Conditions for taking the data were pressures between 228 and 609 kPa and temperatures ranging from 17 to 20 °C.

*Freon-113 loop:* Freon-113 has been shown to be a good fluid to simulate steam-water at nuclear reactor operating conditions. (Lopez de Bertodano et. al., 1998) The Freon loop at 1 MPa simulates the conditions of steam-water at a pressure of 7 MPa quite closely.

The Freon-113 test section is an adiabatic upward flow stainless steel tube with an inner diameter of 10 mm. The Freon loop is similar to the air-water loop in geometry and instrument arrangement. In addition, it uses the same liquid film extraction technique. Further details about the Freon-113 loop may be obtained from Lopez de Bertodano, Assad and Beus (1998). The experimental conditions were pressures between 308 and 1135 kPa and temperatures ranging from 85 to 145 °C.

*Procedure:* The film extraction technique involves the suction of a liquid film through a porous tube by a pressure difference across it. The extraction is performed through a 63 mm long porous tube with a pore size of 100 microns. The design of the extraction probes is based on previous research by Sekoguchi, Tanaka and Ueno (1985) and Cousins

and Hewitt (1968). In our experiment there are two film extractions (see Figure 4). The first extraction measures the film flow rate and the second the deposition rate, or the entrainment rate if they are the same. The length of the porous tubes is larger than the minimum necessary to remove the disturbance waves and the distance between them is short enough to prevent re-entrainment of the second film.

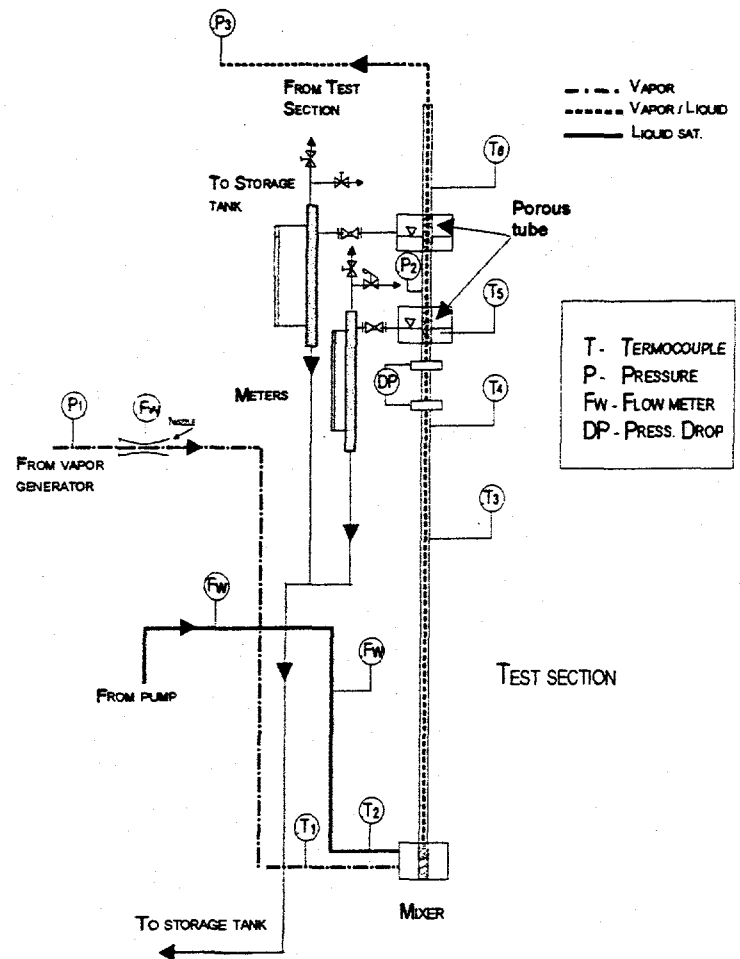


Figure 3: Test section schematic

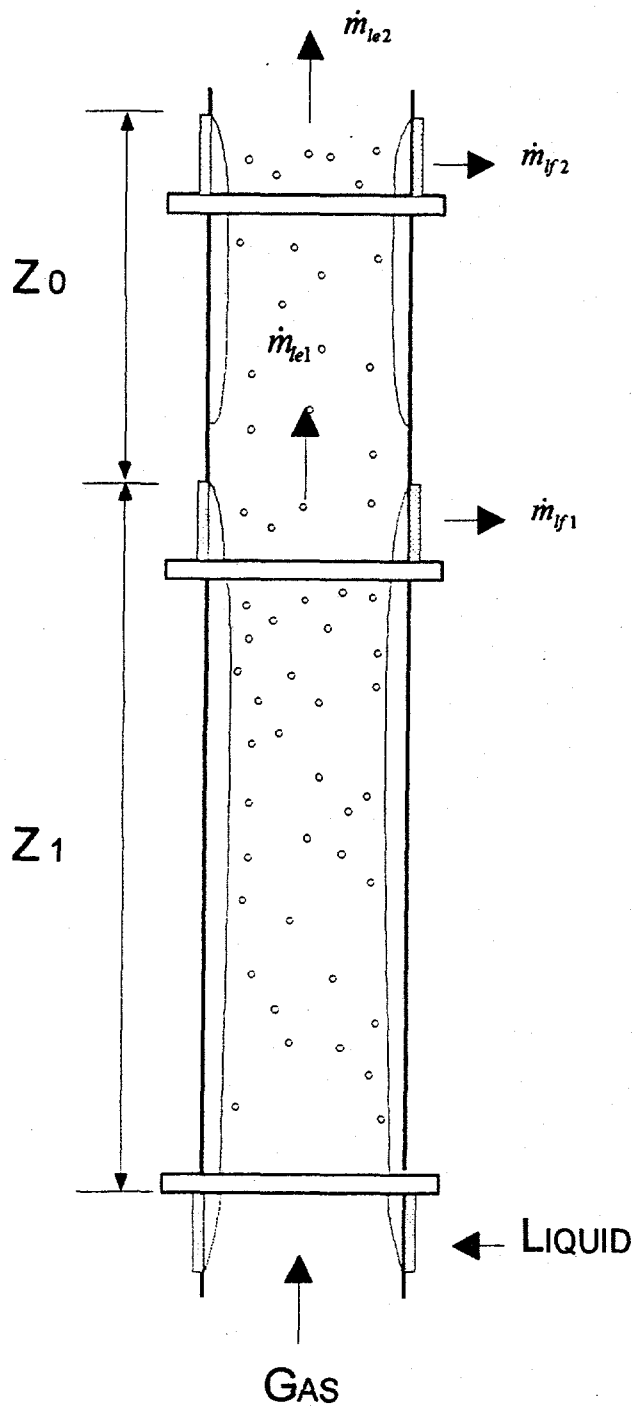


Figure 4: Double extraction technique

For ripple annular flow the entire liquid film is removed at the first extraction. This was checked in the air-water loop where it was seen that the tube right after the extraction had no film in it. After the first extraction the entrained droplets in the gas core deposit on the tube wall for a length of 305 mm in the

air-water loop and 102 mm. in the Freon loop. A new liquid film develops entirely from liquid deposition and a second liquid film extraction is performed.

On the other hand the first extraction cannot remove the entire film when the regime is frothy annular. Dallman et. al. (1979) pointed out that: "with such a short length thick liquid layers with large roll waves (frothy annular flow) possibly could 'wash over' the porous section and be counted as entrained liquid". This is the premise for our ability to measure the transition from ripple to frothy annular flow. When the flow becomes frothy annular the film extraction technique fails. The entire liquid film is not removed at the first extraction unit, but continues on and is extracted at the second extraction unit.

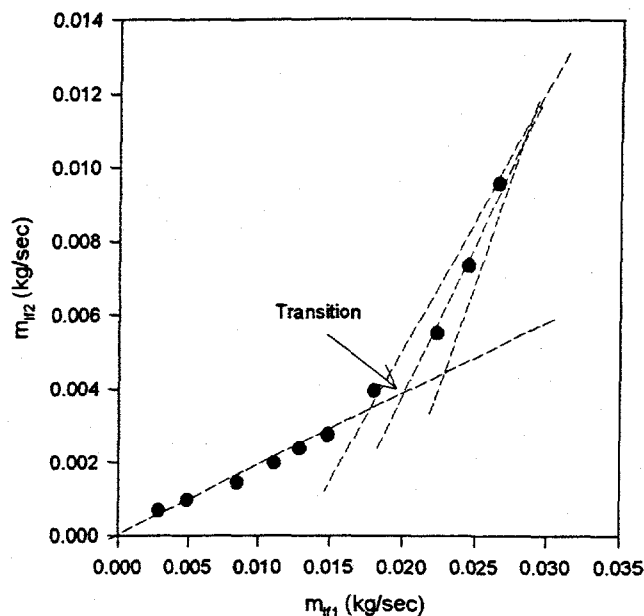


Figure 5: Transition from Ripple to Frothy Annular Flow

Data are obtained keeping the gas flow rate and pressure constant and varying the liquid flow rate at the inlet. A plot is then made of the liquid mass flow rate of the second extraction unit ( $\dot{m}_{f2}$ ) versus the liquid mass flow rate of the first extraction unit

( $\dot{m}_{y1}$ ). The hypothesis of this research is then that the point where the slope changes is the transition point from ripple to frothy annular flow (see Figure 5). At low superficial vapor velocities the transition is characterized by an abrupt change in the slope. As the superficial vapor velocity is increased the slope change becomes less abrupt. Therefore additional errors may occur at the high superficial vapor velocities due to the difficulty in determining the transition point from the small change in the slope.

### MODEL

Figure 6 shows a disturbance wave. It is assumed that frothy flow develops when the disturbance wave breaks. The sketch shows a control volume of height  $k_s$  and length  $\lambda$  on the tube wall,

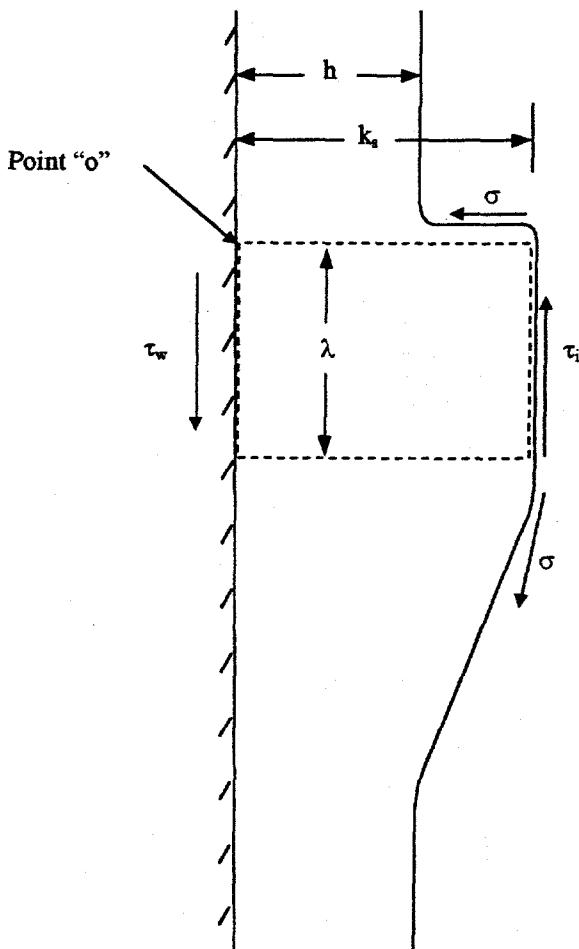


Figure 6: Control volume for disturbance wave model

which are the height and the length of the disturbance wave respectively. The surface forces are the surface tension force, the wall shear force  $\tau_w$  and the interfacial shear force  $\tau_i$ . The gravitational force is neglected.

The proposed model is developed for the purpose of scaling the transition from ripple to frothy annular flow. It provides the necessary functional groups and their appropriate relationships. The result is a dimensionless expression of the form:

$$f\left(We_g, \frac{We_f}{Re_f^{0.2}}\right) = 0 \quad (1)$$

To begin with the sum of the moments around point "o" in Figure 6 is:

$$\tau_i \lambda k_s \cong \sigma k_s \quad (2)$$

This can be simplified to:

$$\tau_i \cong \frac{\sigma}{\lambda} \quad (3)$$

If we assume that  $\lambda$  is proportional to  $k_s$  and we multiply by  $D/D$  then equation (3) becomes:

$$\tau_i \frac{D}{\sigma} \frac{k_s}{D} \cong \text{Constant} \quad (4)$$

In order to solve equation (4), we need to determine expressions for the interfacial shear force,  $\tau_i$ , and for  $k_s/D$ . First, an expression for the interfacial shear force,  $\tau_i$ , was obtained starting from Wallis' correlation (1969):

$$\tau_i = \frac{C_i \rho_g j_g^2}{2} \quad (5)$$

$$C_i = 0.005 \left(1 + 75 \frac{k_s}{D}\right) \quad (6)$$



Inserting equation (6) into equation (5) and assuming that  $75 \frac{k_s}{D} \gg 1$  one obtains:

$$\tau_i \propto \frac{k_s}{D} \rho_g j_g^2 \quad (7)$$

Wallis made the assumption that  $k_s \cong 4h$ , where  $h$  is the film thickness. Replacing  $k_s$  by  $h$ , and inserting equation (7) in equation (4) yields:

$$\frac{D \rho_g j_g^2}{\sigma} \frac{h^2}{D^2} \cong \text{Constant} \quad (8)$$

Equation (8) may be simplified using the definition of the non-dimensional Weber gas number:

$$\text{We}_g \frac{h^2}{D^2} \cong \text{Constant} \quad (9)$$

Now an expression must be developed for  $\frac{h}{D}$  in equation (9). To determine this expression let us begin with a correlation for the film thickness,  $h^+$ , by Henstock and Hanratty (1976):

$$h^+ = \frac{hu^*}{\nu_f} = 0.0379 \text{Re}_f^{0.9} \quad (10)$$

In equation (10)  $u^*$  is the friction velocity:

$$u^* \cong \sqrt{\frac{\tau_i}{\rho_f}} \quad (11)$$

Inserting equation (11) into equation (10) and multiplying by  $\frac{D}{D}$ , we can now solve for  $\frac{h}{D}$ .

$$\frac{h}{D} \cong \frac{\nu_f \text{Re}_f^{0.9}}{D \sqrt{\frac{\tau_i}{\rho_f}}} \quad (12)$$

Now inserting the expression for the interfacial shear,  $\tau_i$ , i.e.: equation (7), into equation (12) yields:

$$\frac{h}{D} \cong \left( \frac{\nu_f \text{Re}_f^{0.9}}{D} \frac{1}{j_g} \sqrt{\frac{\rho_f}{\rho_g}} \right)^{2/3} \quad (13)$$

The first term on the right hand side,  $\left( \frac{\nu_f \text{Re}_f^{0.9}}{D} \right)$ ,

can be rewritten as  $\frac{1}{\text{Re}_f^{0.1}} j_f$ . Using this and

rearranging equation (13), we obtain:

$$\frac{h}{D} \cong \left( \frac{1}{\text{Re}_f^{0.2}} \frac{\rho_f j_f^2}{\rho_g j_g^2} \right)^{1/3} \quad (14)$$

The last two terms on the right hand side of equation (14) can be written as non-dimensional Weber numbers of the liquid film and gas:

$$\frac{h}{D} \cong \left( \frac{1}{\text{Re}_f^{0.2}} \frac{\text{We}_f}{\text{We}_g} \right)^{1/3} \quad (15)$$

Now that an expression for  $\frac{h}{D}$  is obtained we can substitute equation (15) into equation (9):

$$\text{We}_g \left( \frac{1}{\text{Re}_f^{0.4}} \frac{\text{We}_f^2}{\text{We}_g^2} \right)^{1/3} \cong \text{Constant} \quad (16)$$

Equation (16) may be rewritten in final form as:

$$\text{We}_g \frac{\text{We}_f^2}{\text{Re}_f^{0.4}} \cong \text{Constant} \quad (17)$$

This result allows us to identify the appropriate dimensionless numbers already given in equation (1).

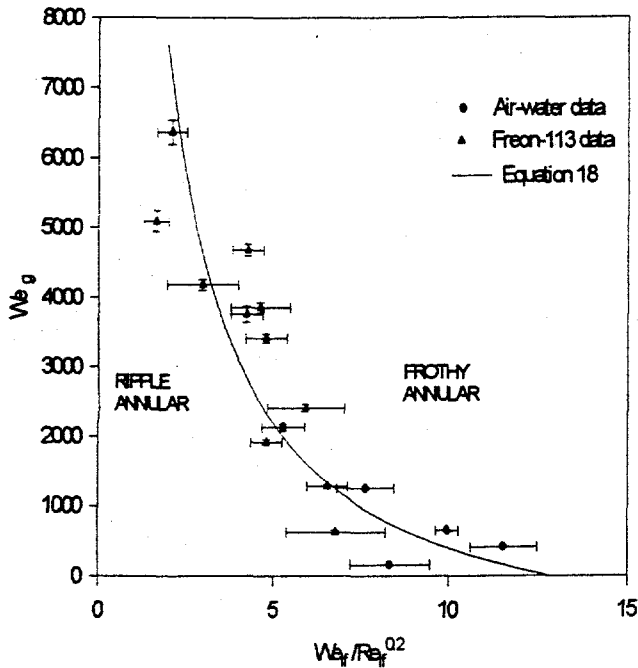


Figure 7: Comparison of data and model

## RESULT

Using the previous model we are able to describe the transition from ripple to frothy annular flow in physical terms. Figure 7 shows the plot of the air-water and Freon-113 data that was obtained in this study in terms of the dimensionless numbers of equation (1). A good fit to these data was obtained with the correlation:

$$We_g = \frac{18000}{\frac{We_f}{Re_f^{0.2}}} - 1400 \quad (18)$$

The flow must be annular to begin with, so this correlation must be used together with an annular flow transition criterion such as Mishima and Ishii's (1984):

$$j_g \geq \frac{\sigma g (\rho_f - \rho_g)}{\rho_g^2} N_{hf}^{-0.2} \quad (19)$$

where

$$N_{hf} = \frac{\mu_f}{\left( \rho_f \sigma \sqrt{\frac{\sigma}{g(\rho_f - \rho_g)}} \right)^{1/2}} \quad (20)$$

If equation (19) is satisfied and if  $We_g$  obtained from equation (18) is larger than the actual value, then the flow is "ripple annular", but if it is smaller the flow is "frothy" annular.

An uncertainty analysis was performed for each of the functional groups in equation (18). From this we obtained vertical uncertainty bars (i.e.:  $We_g$ )

and horizontal uncertainty bars (i.e.:  $\frac{We_f}{Re_f^{0.2}}$ ).

**Vertical error bars:** For the air-water loop the two important sources of uncertainty of  $We_g$  are the inlet flow rate ( $\dot{m}_g$ ) and the inlet air pressure ( $P_{in}$ ), which can be expressed in the following manner:

$$\frac{\Delta We_g}{We_g} = \sqrt{\left( \frac{\Delta \dot{m}_g}{\dot{m}_g} \right)^2 + \left( \frac{\Delta P_{in}}{P_{in}} \right)^2} \quad (21)$$

With an uncertainty of  $\pm 2\%$  for each term the total uncertainty for  $\frac{\Delta We_g}{We_g}$  is  $\pm 2.8\%$ . For the Freon data

the dominant uncertainty comes from condensation in the test section ( $\dot{m}_{cond.}$ ). This condensation was estimated from film extraction data with pure vapor flow at the inlet. The resulting uncertainties in  $We_g$  are no greater than 3.9%.

**Horizontal error bars:** The uncertainty  $\Delta \left( \frac{We_f}{Re_f^{0.2}} \right)$

depends primarily on the uncertainty of the position of the first extraction flow measurement where the transition takes place (i.e.: the "elbow" in Figure 5):

$$\frac{\Delta \left( \frac{We_f}{Re_f^{0.2}} \right)}{\frac{We_f}{Re_f^{0.2}}} = \frac{1.8 \Delta \dot{m}_f}{\dot{m}_f} \quad (22)$$

Furthermore for the Freon data another source of uncertainty is the condensation rate. The total uncertainties for both experiments were reasonably low, ranging from 6.2% to 26.6% and averaging 15.7%. More details about the uncertainty analysis are given by Helm (1998).

## CONCLUSION

The limit of validity of the film extraction technique was obtained experimentally. Thus the limit of the supporting data for the entrainment rate correlation proposed by Lopez de Bertodano et. al. (1998) is identified. Furthermore this limit coincides with a flow regime transition from ripple to frothy annular flows.

A model was obtained for this limit given by equation (18). This model collapses the experimental data for air-water and Freon-113, thus providing a general prediction that may be used for high pressure steam-water flows in small diameter channels (i.e.: 10 mm) because it has been validated for similar physical properties (e.g.: surface tension and density ratio).

## REFERENCES

- Bennett, A. W., Hewitt, G. F., Kearsey, H. A., Keeys, R. K. F. and Lacey, P. M. C., "Flow Visualization Studies of Boiling at High Pressure", *Proc. Inst. Mech. Eng.*, 180, (Part 3C), 260, 1965-1966.
- Cousins, L. B. and Hewitt, G. F., "Liquid phase mass transfer in annular two-phase flow: droplet deposition and liquid entrainment," *United Kingdom Atomic Energy Authority, AERE-R5657*, 1968.
- Dallman, J. C., Jones, B. G., Hanratty, T. J., "Interpretation of Entrainment Measurements in Annular Gas-Liquid Flows", *Two Phase Momentum, Heat and Mass Transfer in Chemical Process and Engineering Systems*, vol. 2, p. 690, Durst, F. And Afgan, N., (ed.), Hemisphere Publishing Co., Washington, D. C., 1979.
- Henstock, W. H. and Hanratty, T. J., "The interfacial drag and the height of the wall layer in annular flows", *AIChE Journal*, vol. 21, No. 6, p. 990, 1976.
- Helm, D. E., "Transition of Ripple to Frothy Annular Flow in Vertical Upward Flow," M.S. thesis, Purdue University, West Lafayette, Indiana, 1998.
- Hewitt, G. F. and Roberts, D. N., "Studies of Two-Phase Flow Patterns by Simultaneous X-Ray and Flash Photography", *United Kingdom Atomic Energy Authority, AERE-M 2159*, p. 1, 1969.
- Lopez de Bertodano, M. A., Assad, A. and Beus, S., "Entrainment rate of droplets in the ripple-annular regime for small vertical ducts," *Nuclear Science and Engineering*, vol. 129, p. 72, 1998.
- Lopez de Bertodano, M. A., Jan, C. S. and Beus, G., "Annular Flow Entrainment Rate Experiment in a Small Vertical Pipe," *Nuclear Engineering and design*, vol. 178, p. 61, 1997.
- Mishima, K., and Ishii, M., "Flow Regime Transition Criteria for Upward Two-Phase Flow in Vertical Tubes," *Int. J. Heat and Mass Transfer*, vol. 27, n. 5, p. 723, 1984.
- Sekoguchi, K., Tanaka, O., and Ueno, T., "On the determination method of entrained droplet flow rate in disturbance wave region of annular flow," *Bulletin of JSME*, vol. 28, No. 240, p. 1105, 1985.
- Wallis, G. B., "One-dimensional Two Phase Flow", McGraw-Hill, New York, 1969.